# Unusual softening of interfaces in superlattice thin films: Proposal of the interface elasticity parameter

H. Ogi, T. Shagawa, N. Nakamura, M. Hirao
*Graduate School of Engineering Science, Osaka University, Toyonaka, Osaka 560-8531, Japan*

Corresponding author: H. Ogi*
(Dated: July 14, 2009)

We propose theoretical and experimental model to extract the interface elastic stiffness in superlattice thin films using picosecond ultrasound spectroscopy. Ultrafast light pulses excite and detect thickness phonon vibrational modes in a five-layered multilayer film, consisting of three matrix layers and two ultrathin interlayers. The thickness of the interlayer is varied between 2 and 10 Å. We define the interface elasticity parameter as the ratio of the resonance frequencies of the two phonon modes, which are sensitive and insensitive to the interface elastic constants, and inversely evaluated the elastic stiffness of the interlayer. Using Pt as the matrix and Co, Fe, and Pd as the interlayer materials, we evaluate their interface stiffness, which is considerably lower than the bulk value.

PACS numbers: 62.20.Dc, 68.35.Iv, 78.47.+p, 61.72.-y

The evaluation of the interfacial elastic stiffness has been of capital importance for understanding mechanics superlattice thin films. Clemens and Eesley [5] measured the out-of-plane longitudinal-wave modulus in multilayer thin films using picosecond-ultrasound pulse-echo method. They observed significantly lowered macroscopic stiffness when the bilayer thickness of the multilayer is smaller than ∼50 Å and attributed this phenomena to the elongation of the lattice near the interfaces, referring to the relationship between the surface energy and the lattice elongation [6]. Nakamura *et al.* [7] measured the anisotropic elastic constants of Co-Pt multilayer films using resonance ultrasound spectroscopy and suggested the elastic anisotropy caused by the elastic strain. They also showed correlation of the out-of-plane modulus with PMA in the Co-Pt binary system, and indicated that defects dominated both the macroscopic stiffness and PMA [4]. However, all the previous works measured the macroscopic elastic stiffness, to which the interfacial stiffness poorly contributes because of the small volume fraction. The macroscopic stiffness is easily affected by the stiffness of the individual layers, the defects inside the layer, noncrystalline regions, and so on. Therefore, it has never been straightforward to correctly evaluate the interface stiffness.

Here, we propose a model to extract the interface stiffness in a superlattice thin film using different standing-wave phonon modes. When the acoustic impedance of the substrate is smaller than that of the bottom layer of the superlattice film, standing waves with nearly free boundaries occur within the multilayer thin film. We focus two modes which are sensitive and insensitive to the interface stiffness. The ratio of their resonance frequencies reflects the interface stiffness, while it is basically independent of the other factors (stiffness, density, and thickness of individual layers, defects and noncrystalline phases inside layers, and the boundary adhesion with the substrate). We define the interface elasticity parameter (IEP) as the ratio of the resonance frequencies.

The interface structures have been evaluated in detail by the reflection high-energy electron diffraction (RHEED) method during the deposition procedure [8]. In the case of superlattice films with immiscible atomic layers, many misfit dislocations are introduced, causing incoherent interfaces, and they will deteriorate the bond strength at the interface. In multilayer films with miscible atomic layers, however, coherent interfaces can be made, and the atomic layers near the interfaces are highly strained. For example, in the systems of Co-Pt and Au-Cu multilayer films, the in-plane strains in the thin layers (Co and Au layers, respectively) are relaxed by about 10 atomic layers (or ∼20 Å) from the interface [9, 10]. Therefore, an ultrathin layer thinner than ∼10 Å in multilayer films reflects essential properties of the interface. We thus use the five layered multilayer film with two ultrathin atomic layers between three thicker matrix layers. As the matrix material, we use Pt. As the interlayer, we select Co, Fe, and Pd.

We calculate the phonon vibrational modes for the longitudinal wave in a multilayer system consisting of $n$ layers ($n$=1 shows the top layer). Taking the $z$ axis perpendicularly to the surface from the top surface of the film toward the substrate, the partial plane waves in the individual layers are expressed by $u_i^{(\pm)} = A_i^{(\pm)} e^{\mp j k_i z}$, where $k_i = \omega\sqrt{\rho/C_i}$. Here, we omit showing the term $e^{j\omega t}$ considering the harmonic vibration. $u_i$ and $A_i$ denote the displacement and the complex amplitude in the $i$th layer, respectively. The superscripts (+) and (-) represent quantities for the partial plane waves propagating toward the positive and negative directions of the $z$ axis, respectively. $k_i$ is the wavenumber at the $i$th layer. $C_i$ and $\rho_i$ are the out-of-plane longitudinal-wave elastic modulus and the mass density at the $i$th layer, respectively. Considering free boundaries at both sur-

faces, the boundary conditions for continuity of the displacement and the stress yield an eigenvalue problem $\Gamma\mathbf{A}$=0 with a matrix $\Gamma$ of $(2n)\times(2n)$ [**?** ]. The vector $\mathbf{A}$= $(A_1^{(+)}, A_2^{(+)}, ..., A_n^{(+)}, A_1^{(-)}, A_2^{(-)}, ..., A_n^{(-)})$ consists of the complex amplitudes, representing the amplitude and phase of displacement. Thus, resonance frequencies of the $n$-layered multilayer film are obtained from the eigenvalues of the matrix $\Gamma$ by solving det[$\Gamma$]=0.

We focus on two vibrational modes in a five-layered system which is symmetric about the middle plane; it consists of the three thicker matrix layers of Pt and two ultrathin interlayers. For example, Figure 1 shows stress ($\sigma_{33}$) and displacement distributions of fundamental and second thickness-resonance modes for a superlattice film of Pt(70 Å)/Co(10 Å)/Pt(140 Å)/Co(10 Å)/Pt(70 Å). The absolute value of the normal stress of the second mode takes the maxima at the interlayers, which is larger than the stress at the interlayers of the fundamental mode by a factor 3 when the displacement amplitude is the same. Therefore, the elastic constant near the interface region affects the second-mode resonance frequency $f_2$ more efficiently than the fundamental-mode one $f_1$. We here propose the interface elasticity parameter (IEP) defined by

$$\mathrm{IEP} = \frac{f_2}{2f_1}. \tag{1}$$

IEP becomes larger as the interface stiffness increases, and it equals 1 for a uniform monolayer.

We use Pt for the matrix layers because of two reasons. First, Pt thin films show smooth surfaces ($R_a$ <∼5 Å) and dense structures, and their elastic constants are close to the bulk value [11], making the analysis easier. Second, Pt produces coherent interfaces with Co [4, 9], making a good model to compare the elastic stiffness of tightly bonded interface (Pt-Co) with other interfaces. As the interlayer materials, we select Co for making coherent interfaces, and Fe and Pd as well.

We deposited superlattice thin films on (001) Si substrates by the magnetron-sputtering method. The substrates were cleaned in the piranha solution (98%$H_2SO_4$:33%$H_2O_2$=4:1) before deposition. The film thickness was determined from the sputtering rates of individual target materials: We performed the x-ray total reflectivity measurement [12] individually for the target materials to calibrate the sputtering rate in advance. For evaluating the structure, we performed the high-angle x-ray diffraction (XRD) measurement. The total thicknesses of the multilayer films were about 290 Å; the middle Pt layer was 140 Å thick, and the top and bottom Pt layers were 70 Å thick. The thickness of two interlayers between them was between 2 and 10 Å.

The picosecond ultrasound method was established by Thomsen *et al.* [14, 15] for the first time. The thin film specimen is illuminated by an ultrafast pump light pulse to excite subterahertz phonons. The time-delayed probe light pulse then enters the film to detect the phonon vibrations from the change in its reflectivity. When the film is thinner (<∼300 Å), non-propagating phonon modes ($\Gamma$ point vibrations) occur [**?** ], providing oscillations in the reflectivity change, from which the elasticity of ultrathin films were evaluated [11, 20]. These previous works, however, focused only on the fundamental resonance mode, neglecting the importance of the second mode. In this study, we actively use the second mode for the interface elasticity. Details of our optics appear elsewhere [11, 13].

Figure 2 shows typical time-resolved reflectivity changes of the probe light and the corresponding Fourier spectra for a Pt monolayer and multilayer thin films. We clearly observe oscillations from all multilayer thin films, and three peaks in their Fourier spectra at ∼70, ∼140, and ∼230 GHz. The last peak (∼230 GHz) corresponds to Brillouin oscillation from the Si substrate, which is caused by diffraction of the probe light pulse in the Si substrate by the acoustic phonon pulse propagating in Si [21, 22]. (This peak overlaps the third thickness resonance peak, deteriorating the peak shape.) The first two peaks indicate the $\Gamma$ point phonon vibrations within the thin films. In Fig. 2(b), the resonance frequency of the second mode is lowered in the multilayer thin films involving the 2-Å-thick Fe interlayers, indicating lowered interface stiffness.

We obtained the IEP values for various multilayer thin films and inversely determined the elastic stiffness of the ultrathin interfaces as followed. First, we calculated the IEP values by solving the eigenvalue problem of the $\Gamma$ matrix using the elastic constants of corresponding bulk materials. Because the XRD spectra (not shown) showed strong (111) texture of Pt, we considered the complete (111) texture for the Pt matrix layers, and (0001), (110), and (111) texture for Co, bcc-Fe, and Pd layers, respectively, assuming that their closed-packed planes are parallel to the film surface. Pt, Co, and Pd layers are transversely isotropic in the film plane, and their out-of-plane longitudinal-wave moduli $C$ are obtained from the monocrystal elastic constants $C_{ij}$ as $C = (C_{11} + 2C_{12} + 4C_{44})/3$=384.7, $C = C_{33}$=335, and $C = (C_{11} + 2C_{12} + 4C_{44})/3$=288.7 GPa for Pt, Co, and Pd layers, respectively. Because a [110]-oriented Fe grain shows tetragonal elastic symmetry, we averaged the elastic constants in the plane about the [110] direction to deduce the transversely isotropic elastic constants of the (110)-texture bcc-Fe layer (in-plane Hill averaging method [24]). This procedure yields $C$=290.6 GPa for the Fe layer. Second, we determined the interlayer stiffness inversely by fitting the theoretical IEP value to the measured one. IEP depends on stiffnesses, mass densities, and thicknesses of Pt layer and interlayer. Therefore, we inversely determined the stiffness of the interlayer using bulk values for the Pt stiffness, and mass densities and thicknesses of Pt and interlayer material. The simplex method was adopted to perform this calculation. The

results for independent measurements for different specimens are shown in Fig. 3(a), where the horizontal axis is the interlayer elastic constant normalized by the corresponding bulk value. Thus, the interfacial stiffness is highly lowered in the multilayer films.

We show higher sensitivity of the interface stiffness to the IEP value than the other parameters. The difference between the measured and predicted IEP values is as large as ∼6%. Possible factors affecting IEP are not only the interlayer stiffness, but also the matrix-layer stiffness, and mass densities and thicknesses of the matrix layer and interlayer. For evaluating their contributions, we calculated sensitivities of those parameters to IEP numerically, which are shown in Table I. Among the parameters investigated, the interlayer stiffness is the primary cause for the large decrement of the IEP value. A 10% fluctuation in the thickness of the interlayer or the matrix layer, for example, would cause only ∼0.2% change in the IEP value, which is much smaller than the observed IEP change. Because the film thickness was carefully controlled based on the x-ray reflectivity measurement, the film thickness error is expected to be less than 5%. Also, an increase in the Pt-layer stiffness can cause a decrease in the IEP value. Our previous study actually revealed that the ultrathin Pt film was stiffened when the thickness was smaller than ∼100 Å, but the increment is ∼10% at most [11], which would decrease the IEP value by <∼0.4%. The sensitivity of IEP to the mass density is lower, and it is unrealistic that the change of the mass density decreased the IEP value so significantly. The change in IEP from the theoretical value is therefore principally caused by the change in the interlayer stiffness.

Figure 4(b) shows the interlayer elastic constant as well as the elastic constant of the 280-Å-thick Pt monolayer. The elastic constant of the Pt monolayer is lower than the bulk value by about 6%, which is attributed to the non-perfect (111) texture of Pt. The reproducibility of the measurement of IEP for a single specimen was good enough (<∼1%), but it was poor among different specimens deposited even with an identical condition. We attribute this discrepancy to the different interlayer structure, not to the measurement ambiguity: The interlayer structure will be easily affected by the surface condition of the substrate and slight transition of the sputtering condition. Nevertheless, Figure 3(b) shows that the interlayer stiffness in the multilayer film is significantly lower than the bulk value, and this trend is enhanced in thinner interlayers. For example, the stiffness of 2-Å-thick Fe layer is only 20% of the bulk value. Such an extraction of the interfacial stiffness has not been made possible so far.

Elastic softening in multilayer films has been attributed to the interfacial strain [5, 25]. We then estimate the in-plane strain in the interlayer from the continuum mechanics, assuming an in-plane stress field and coherent interfaces. The in-plane strain stored in a 10-Å-thick interlayer is calculated to be 0.10, 0.072, 0.0083, and -0.031 for Co, fcc-Fe, Pd, and bcc-Fe, respectively, when the total thickness of the Pt layer is 280 Å. (We used lattice misfit strains at the closed-packed planes of 0.11, 0.076, 0.0085, and -0.032, respectively.) From this calculation, we consider that the softening of interface is principally caused by defects such as interfacial dislocations, rather than the strain, because the Co interlayers show higher stiffness than Fe and Pd layers despite that they should be highly strained: It is known that Co and Pt layers bind coherently each other, and the large lattice-misfit strain should be involved in the Co interlayer. Coherence of their interfaces was confirmed directly by RHEED measurement [8, 9] and indirectly by the PMA measurement [4]. (The interfacial strain is needed for achieving high PMA.)

Based on picosecond ultrasound spectroscopy, we presented a parameter, interfacial elasticity parameter (IEP), for evaluating interfacial stiffness of a superlattice film. In the case of the 5-layered multilayer model, the second resonance mode shows the maximum sensitivity at the ultrathin interlayers, providing the enhanced stiffness information there, while the elastic properties in the matrix layer can be made negligible by taking the ratio between the fundamental and the second modes' resonance frequencies. The IEP value was significantly smaller than the predicted value in multilayer thin films with Co, Fe, and Pd interlayers in the Pt matrix layers. We inversely calculated the interface stiffness, which showed highly softened interlayers. This trend is remarkable for the thinner interlayers. The 2-Å-thick Fe interlayer, for example, shows the stiffness of only 20% of the bulk value. Considering that the interface with Co interlayer showed higher stiffness than other interlayers, the softened interlayer is attributed to the interfacial defects, not the interfacial strain, because Co layers should be most strained.

* Electronic address: ogi@me.es.osaka-u.ac.jp

[1] P. F. Carcia, J. Appl. Phys. 63, 5066 (1988).
[2] T. Kingetsu, J. Appl. Phys. 76, 4267 (1994).
[3] N. Nakamura, H. Ogi, T. Ono, and M. Hirao, Appl. Phys. Lett. 86,111918 (2005).
[4] N. Nakamura, H. Ogi, T. Yasui, M. Fujii, and M. Hirao, Phys. Rev. Lett. 99, 035502 (2007).
[5] B. M. Clemens and G. L. Eesley, Phys. Rev. Lett. 61, 2356 (1988).
[6] J. K. Rose, J. R. Smith, and J. Ferrante, Phys. Rev. B 28, 1835 (1983).
[7] N. Nakamura, H. Ogi, T. Ono, and M. Hirao, J. Appl. Phys. 97, 013532 (2005).
[8] T. Kingetsu, Y. Kamada, and M. Yamamoto, Sci. Tech. Adv. Mater. 2, 331 (2001).
[9] K. Nishikawa, T. Kingetsu, K. Sakai, T. Kurumizawa, and M. Yamamoto, J. Magnet. Magnet. Mater. 126, 153 (1993).
[10] Y. Kamada, T. Kingetsu, H. Kasai, and M. Yamamoto, J. Magnet. Magnet. Mater. 198/199, 707 (1999).
[11] H. Ogi, M. Fujii, N. Nakamura, T. Yasui, and M. Hirao, Phys. Rev. Lett. 98, 195503 (2007).
[12] L. Parratt, Phys. Rev. 95, 359 (1954).
[13] H. Ogi, M. Fujii, N. Nakamura, T. Shagawa, and M. Hirao, Appl. Phys. Lett. 90, 191906 (2007).
[14] C. Thomsen, J. Strait, Z. Vardeny, H. J. Maris, J. Tauc, and J. J. Hauser, Phys. Rev. Lett. 53, 989 (1984).
[15] C. Thomsen, H. T. Grahn, H. J. Maris, and J. Tauc, Phys. Rev. B 34, 4129 (1986).
[16] H. T. Grahn, H. J. Maris, J. Tauc, and K. S. Hatton, Appl. Phys. Lett. 53, 2281 (1998).
[17] T. C. Zhu, H. J. Maris, and J. Tauc, Phys. Rev. B 44, 4281 (1991).
[18] A. Devos and C. Lerouge, Phys. Rev. Lett. 86, 2669 (2001).
[19] O. B. Wright, B. Perrin, O. Matsuda, and V. E. Gusev, Phys. Rev. B 64, 081202 (2001).
[20] N. Nakamura, H. Ogi, and M. Hirao, Phys. Rev. B 77, 245416 (2008).
[21] A. Devos and R. Côte, Phys. Rev. B 70, 125208 (2004).
[22] H. Ogi, T. Shagawa, N. Nakamura, M. Hirao, H. Odaka, N. Kihara, Phys. Rev. B 78, 134204 (2008).
[23] J. B. Hartman, Dynamics of Machinery (McGraw-Hill, New York, 1956), p. 96.
[24] N. Nakamura, H. Ogi, and M. Hirao, Acta Mater. 52, 765 (2004).
[25] E. E. Fullerton, I. K. Schuller, F. T. Parker, and K. A. Svinarich, J. Appl. Phys. 73, 7370 (1993).

TABLE I: Influences of elastic constants, thicknesses, and mass densities of the matrix Pt layers and the interlayers on the interfacial elasticity parameter IEP of multilayer films consisting of 70, 140, and 70 Å thick Pt layers and 5 Å interlayers. Values of $a\left(\frac{\partial \mathrm{IEP}}{\partial a}\right) \times 100$ are shown, where $a$ is the longitudinal-wave stiffness $C$, thickness $d$, or mass density $\rho$.

| | matrix layer | | | interlayer | | |
|---|---|---|---|---|---|---|
| interlayer material | $C$ | $d$ | $\rho$ | $C$ | $d$ | $\rho$ |
| Co | -3.63 | 2.26 | -1.39 | 3.65 | -2.25 | 1.39 |
| Fe | -4.08 | 2.87 | -1.23 | 4.10 | -2.85 | 1.22 |
| Pd | -4.14 | 2.30 | -1.87 | 4.16 | -2.29 | 1.85 |

**Figure Caption**

**Fig. 1** Distributions of the normal stress ($\sigma_{33}$) (solid line) and the displacement (broken line) at (a) fundamental and (b) second modes in the five layered multilayer film, consisting of Pt(70 Å)/Co(10 Å)/Pt(140 Å)/Co(10 Å)/Pt(70 Å). The vertical broken lines indicate the interfaces between Pt and Co layers.

**Fig. 2** XRD spectra (CoK$\alpha$) of the multilayer films consisting of the three thicker Pt layers and the two ultrathin interlayers (Co, Fe, or Pd).

**Fig. 3** (a)Time resolved reflectivity changes of the probe light from the monolayer Pt and the multilayer films involving Co and Fe layers. The slowly decreasing backgrounds are subtracted using low-order polynomial functions. (b) The corresponding Fourier spectra of the waveforms of (a). BO denotes the Brillouin-oscillation peak. In this figure, the frequency of the multilayer films is adjusted by multiplying a constant so as to match the fundamental resonance frequency with that of the Pt monolayer for emphasizing the changes in the second-mode resonance frequencies of the multilayer films. (Note that $f_1$ varies depending on the total thickness.)

**Fig. 4** (a)Measured (plots) and calculated (lines) IEP values for the multilayer films consisting of the five layers. Solid circles, darkened triangles, and open cubes are measurements for multilayer films with Co, Fe, and Pd ultrathin films. Open triangles are measurements of the multilayer film with Fe layers post-annealed at 773 K. (b)Inversely determined interlayer stiffness of various specimens. Each plot represents individual measurement, and the solid lines are theoretical curves. $C_{bulk}$ denotes the out-of-plane longitudinal-wave modulus of the bulk for the corresponding interlayers.

**Fig. 5** Changes in the low-angle x-ray reflectivity spectrum and IEP values caused by the post-annealing procedure. Solid lines are measurements, and broken lines are fitted theoretical curves. For the as-deposited specimen and the specimen annealed at 573 K, the five-layered model was fitted. For the specimen annealed at 773 K, the monolayer mode was used to fit the theory.

**Fig. 6** Interlayer stiffness for various multilayer thin films as well as the stiffness of 280-Å-thick Pt monolayer.

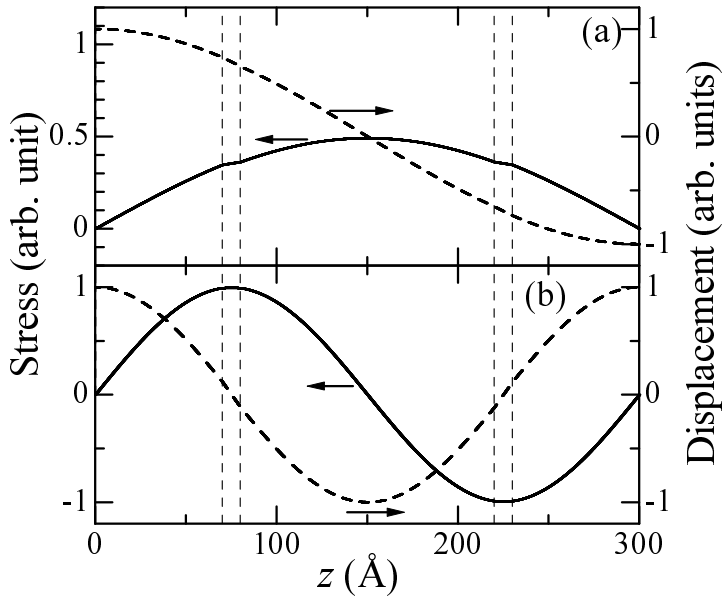
(a)
(b)
Stress (arb. unit)
Displacement (arb. units)
z (Å)
1
0.5
0
-1
100
200
300

FIG. 1:

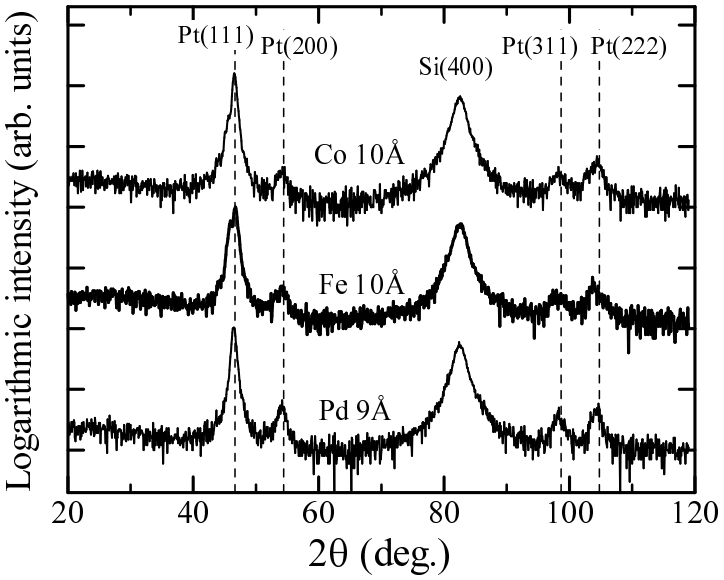
Pt(111)
Pt(200)
Si(400)
Pt(311)
Pt(222)
Co 10Å
Fe 10Å
Pd 9Å
Logarithmic intensity (arb. units)
20
40
60
80
100
120
2θ (deg.)

FIG. 2:

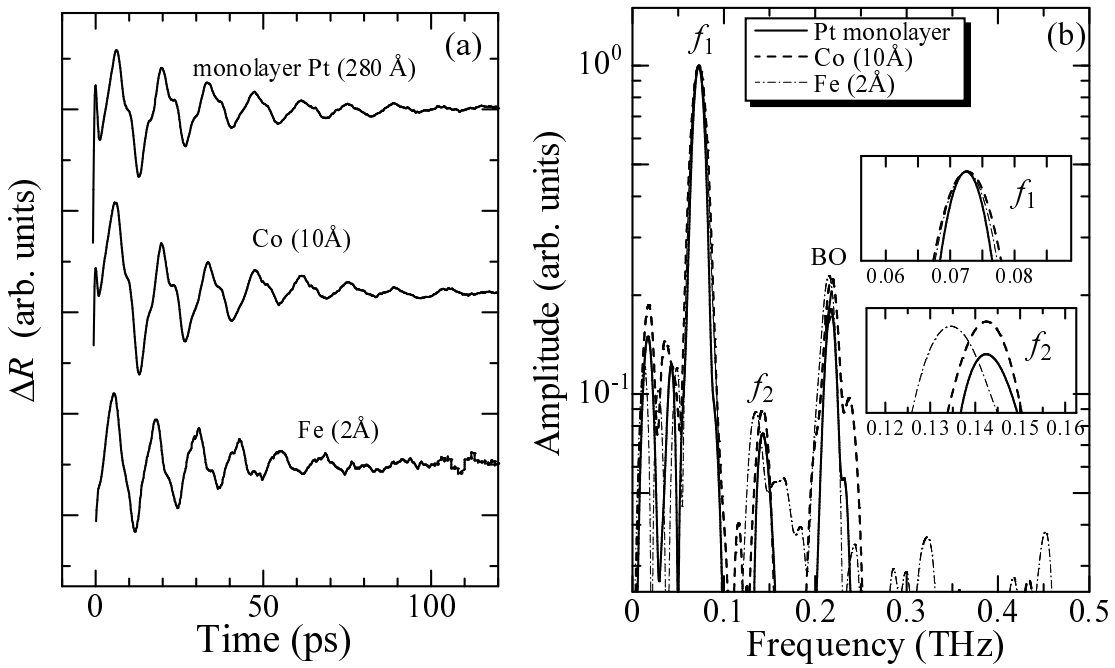
(a)
monolayer Pt (280 Å)
Co (10Å)
Fe (2Å)
ΔR (arb. units)
0
50
100
Time (ps)
(b)
Pt monolayer
Co (10Å)
Fe (2Å)
$f_1$
$f_2$
BO
$10^0$
$10^{-1}$
Amplitude (arb. units)
0
0.1
0.2
0.3
0.4
0.5
Frequency (THz)
0.06 0.07 0.08
0.12 0.13 0.14 0.15 0.16

FIG. 3:

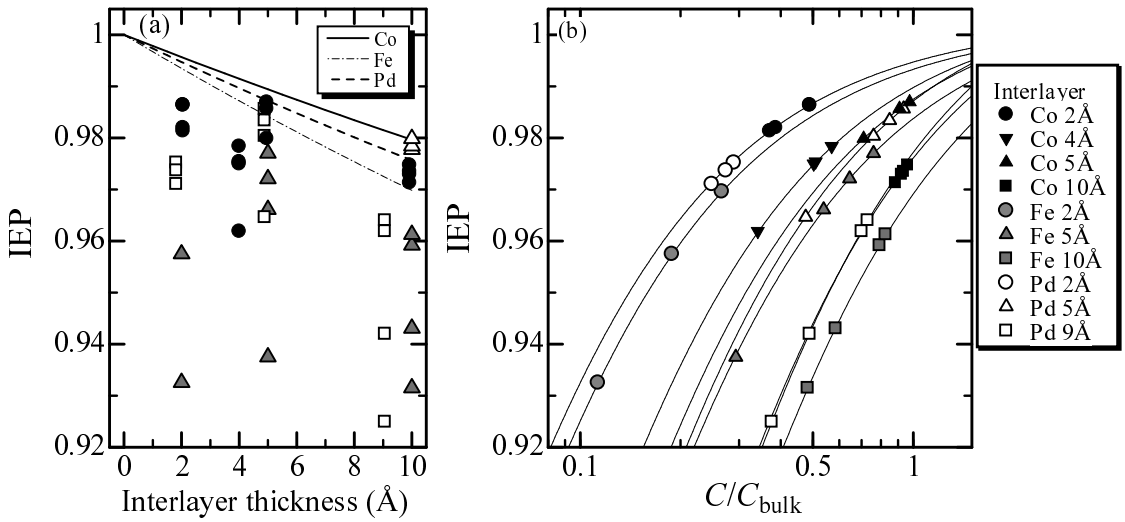
(a)
Co
Fe
Pd
IEP
Interlayer thickness (Å)
(b)
Interlayer
Co 2Å
Co 4Å
Co 5Å
Co 10Å
Fe 2Å
Fe 5Å
Fe 10Å
Pd 2Å
Pd 5Å
Pd 9Å
$C/C_{bulk}$

FIG. 4:

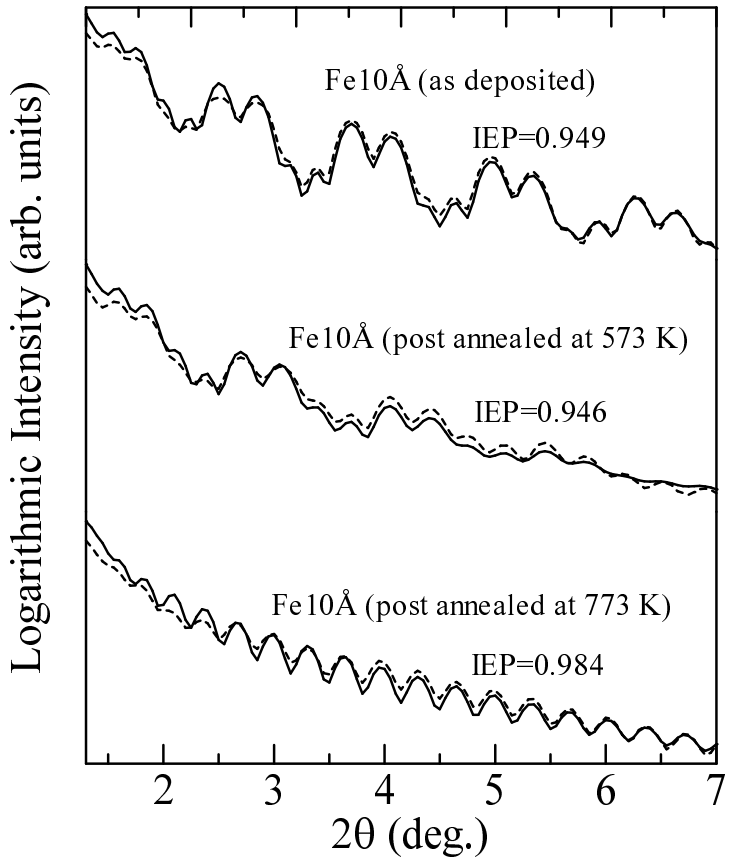
Logarithmic Intensity (arb. units)
Fe10Å (as deposited)
IEP=0.949
Fe10Å (post annealed at 573 K)
IEP=0.946
Fe10Å (post annealed at 773 K)
IEP=0.984
2
3
4
5
6
7
2θ (deg.)

FIG. 5:

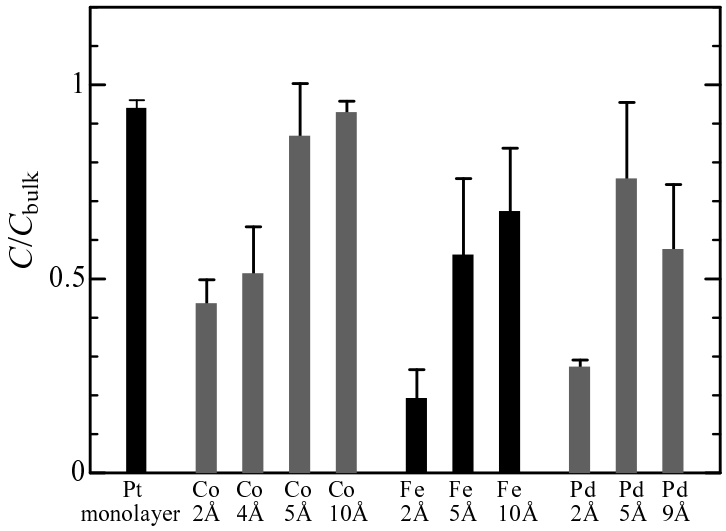
$C/C_{bulk}$
1
0.5
0
Pt monolayer
Co 2Å
Co 4Å
Co 5Å
Co 10Å
Fe 2Å
Fe 5Å
Fe 10Å
Pd 2Å
Pd 5Å
Pd 9Å

FIG. 6: